Soft tissues loadings on healthy knee at different physiological flexions: a coupled experimental-numerical approach

Boris Dousteyssier, Jérôme Molimard, Chafiaa Hamitouche-Djabou, Woo-Suck Han, Eric Stindel

▶ **To cite this version:**

Boris Dousteyssier, Jérôme Molimard, Chafiaa Hamitouche-Djabou, Woo-Suck Han, Eric Stindel. Soft tissues loadings on healthy knee at different physiological flexions: a coupled experimental-numerical approach. Computer Methods in Biomechanics and Biomedical Engineering.Proceedings of the 14th International Symposium CMBBE, Tel Aviv, Israel, 2016, pp.115-128, 2018, Lecture Notes in Bioengineering. hal-02006307

HAL Id: hal-02006307
https://hal.science/hal-02006307v1

Submitted on 4 Feb 2019

HAL is a multi-disciplinary open access archive for the deposit and dissemination of scientific research documents, whether they are published or not. The documents may come from teaching and research institutions in France or abroad, or from public or private research centers.

L'archive ouverte pluridisciplinaire **HAL**, est destinée au dépôt et à la diffusion de documents scientifiques de niveau recherche, publiés ou non, émanant des établissements d'enseignement et de recherche français ou étrangers, des laboratoires publics ou privés.

Soft tissues loadings on healthy knee at different physiological flexions: a coupled experimental-numerical approach

Boris Dousteyssier[a,b,c, d], Jérôme Molimard[a,b,c], Chafiaa Hamitouche[b], Woo-Suck Han[a,b,c], Eric Stindel[b],

[a]Ecole Nationale Supérieure des Mines de Saint-Etienne, CIS-EMSE, F-42023 Saint Etienne, France

[b]INSERM U1059, SAINBIOSE, F-42023 Saint Etienne, France

[c]Université de Lyon, F-69000 Lyon, France

[d] Laboratoire de Traitement de l'Information Médicale, INSERM UMR 1101, 29609 Brest, France

Abstract

Knee degradation and pain when developing osteoarthritis are strongly related not only to the pressure on the cartilage, but also to the knee stability and to the subsequent loadings on the ligaments. Authors proposed the knee models without any flexion. Knee flexion had been introduced by controlling actively muscular groups or by using a full displacement-controlled model. But in both cases, the pressure applied on the articulation has been questioned, the forces used to achieve the flexion being far from the physiology in the former and the bone positioning uncertainties leading to high variations in the cartilage pressure and ligament loads in the latter. Here, we propose a mixed approach, both using medical imaging (MRI, EOS X-ray system) and force platform in conjunction with a finite element model.

A healthy volunteer underwent a MRI and an EOS imaging of the knee. EOS images gave the exact position of the bones for five flexion angles of the knee, ranging from 0° to 85°. The subject's knee was loaded with a specific force on his foot during all acquisitions to keep consistent boundary conditions on the knee. A 3D geometrical model of the bones and cartilages was segmented from the MRI stacks; this model was meshed and smoothed for Finite Element

Analysis (FEA). The bones of the model were fitted to those of the EOS images to have the physiological positions of the knee. The ligaments were then added as truss elements (under tensile forces only). The FEA was carried out according to the experimental boundary conditions (force and flexion angle), so as to ensure the global knee mechanical equilibrium.

To validate this patient-specific model, its bony structure was confronted with the EOS images once the mechanical equilibrium reached. The difference of position was within the error range of the image registration, showing a satisfying equilibrium state. Last, this model gave us an estimation of the tension in the ligaments for every flexion as well as a pressure map on the cartilages.

1. Introduction

2. Method

2.1 EOS acquisition

A healthy volunteer underwent an EOS imaging of the right knee decomposing the movement of climbing a step. Between each acquisition, a 5 cm thick block was added under the foot of the volunteer until the step height of 20 cm was reached. During the whole procedure, a weighting scale was positioned under the foot of the volunteer for him to maintain a constant load of 30 kg. This ensured us the most homogenous boundary conditions possible on the knee at different flexion angles for future simulations. This load has been chosen to be the most comfortable to maintain while being immobile during the whole acquisition procedure. Even though the EOS acquisition is rather quick, approximately 10 seconds per flexion angle, a lighter load had proven to be difficult to control at lower flexion angles and respectively a heavier one was near impossible for higher flexion angles. The data obtained was 5 sagittal and 5 frontal scans of the knee hard tissues at the flexion angles of 0°, 40°, 55°, 70° and 85°. Those images gave us access to the physiological position of the bones at those specific angles of flexion. The schematics of this acquisition and examples of data obtained are shown figure 1.

2.2 Finite Element Analysis

2.2.1 Model geometry and material properties

For the 3D geometrical model of the bones and cartilages used in the simulations to be as complete and physiologic as possible, it was segmented from three different MRI stacks of the volunteer's knee. The MRI modalities used were SPIN echo for the cruciate ligaments insertions, SPIN echo with fat saturation for the lateral ligaments insertions and the cartilages and finally gradient echo for the bones of the articulation. These three MRI stacks had to be fitted one on the other in order for all the different segmented parts to be coherent in the model. The software used for the segmentation was AVISO®. The segmented model was then smoothed using the toolbox GIBBON® for MATLAB® and meshed with Harpoon®. Those different steps in the making of our geometrical model can all be source of uncertainties and so we took especially care that the patient specific aspect of our model was not lost during the process.

The study on the tools used for our model creation was the object of a previous communication *[CMBBE-2015 / paper in progress?]*. It showed that the error between our final geometry and the initial data was less than a millimeter, which is very good considering it is the width of two voxels in the MRI raw data.

In our model, the bones modeled were the tibia and the femur. The patella had been considered unnecessary in a passive stability oriented model. The bones being a lot more rigid than any other materials in the analysis, they were modeled as rigid bodies. The cartilages are viscoelastic tissues; however our analysis being static, the viscosity has no impact in the equilibrium of the model. And thus they were modeled as single-phase linear elastic and isotropic material with an elastic modulus of E = 12 MPa, and a Poisson ratio of ν = 0.45 []. The cartilages are tied to their respective bones, and the contact between the two cartilages is defined as *"hard"*, meaning that no intersection whatsoever is allowed between the two surfaces in contact. A friction coefficient of μ = 0.08 has been implemented. This is the lowest friction coefficient that allowed this first model to achieve and equilibrium at all flexion angles. Finally the ligaments were modeled as truss elements working in tension only, and added on the segmented insertions area. As truss elements they are considered as transversely isotropic. The cross-sectional areas for the ligaments are 42, 60, 18, 25 mm² for respectively the ACL, PCL, LCL and MCL. Longitudinally, they are modeled as hyper-elastic materials following the stress/strain curve given by Weiss and Gardiner []. In the standing position all ligaments has an initial tension of 100 N [], this initial tension has been adjusted to the differences in strain of the different flexion angles and then transferred accordingly. Our geometrical model is shown figure 2.

2.2.2 Simulations

The simulations were carried on ABAQUS®. The goal of each simulation is to recreate the experimental conditions of the EOS data acquisition. In order to do so, the initial bones position of our model was fitted on the physiological positions from the EOS data. We manage to fit our 3D model on two 2D scans with an algorithm which took the contour of a projection of our 3D model then fit and

compare it with the segmented contour of the EOS images. This algorithm is based on the Iterative Closest Point [] in order to fit the two contours, and use the simplex method to find the best match between the possible bone contours from our model with the segmented contours of the EOS images. The fitting precision obtained is 1 mm on the two projected planes and 0.5° along the bone axis. The specifics of the algorithm and an example of contour fitting are shown figure 3.

Once the bones are in their physiological positions for each flexion angles, an intersection between the cartilage of the femur and those of the tibia can be noticed. The analysis consists in removing this intersection, implement the boundary conditions of the experimental setup, reach the global knee mechanical equilibrium, and finally, to validate our model comparing the equilibrium position with the experimental data. All along the analysis, the femur is fixed in space; all degrees of freedom of the tibia are initially locked too. The first step consists in translating the tibia along its axis until there is no more intersection between the cartilages. At this point the contact between the cartilages is implemented and the force on the tibia added: 300 N along its axis. Then all degrees of freedom are released except the rotation in the sagittal plane that is the flexion angle. The FEA is carried out until the global knee mechanical equilibrium. Once achieved, the equilibrium position of the tibia is compared with its initial position to assess the validity of the model. All steps of the FEA are summarized figure 4.

3. Results

The final model is composed of 150 000 elements, mostly in the cartilages. The global knee mechanical equilibrium has been achieved for all simulations except the highest flexion angle, 85°. The following is the results of the four simulations that reached equilibrium.

3.1. Tibia Position

The first result that we seek out was the tibia position. Comparing this position with the initial EOS data ensured us if our model and the global equilibrium it reached are indeed physiological. On figure 5 we can see the distance of each node from their experimental position for the four flexion angles studied, 0°, 40°, 55° and 70°. The simulation at a flexion angle of 0° shows an insignificant distance between the simulation and the experiment for every points of the tibia. The maximum distance observed standing only at 0.7 mm. For the flexion angle of 40° we can also observe that this distance is very small. For 97% of the nodes, their FEA position is at most 2 mm far from their EOS position. The greatest distance observed being 2.66 mm. With the gradient of displacement, we can observe that the difference in positions is due to a rotation along the bone axe, we measured it at 2.6°. On the 55° flexion angle simulation, the distances are ranged from 1.75 mm to 5.24 mm, with 81% of the nodes at less than 4 mm. Once again we can see that those differences are due to a rotation, this time mainly on the frontal plane, we measured it at 3.7°. Finally for the flexion angle of 70°, the distances observed are between 4.0 mm and 5.2 mm. Here the principal cause of displacement is an anterior translation, the displacement component along this axis ranging from 3.8 mm to 5.0 mm.

3.2 Cartilages pressure map

On figure 6 are shown the different pressure map for the four simulations. We can see that in each case the pressure is rather balanced on the two condyles, with a slight overpressure on the external condyle. Furthermore the point of maximum pressure follows the line of contact described in other studies []. The maximum pressure for the different flexion angles are 3.43, 5.34,

5.89 and 5.23 MPa for respectively 0°, 40°, 55° and 70°. We can also notice that the area under pressure slightly decrease when we move to higher flexion angles.

3.3 Ligament stress

Finally the last result on which we focused is the ligaments stress repartition depending on the flexion angle. As shown figure 7, we can see that at the lowest flexion angle the collaterals ligaments withstand the more stress, with their maximum stress at a flexion angle of 0° being 12.07 and 7.37 MPa for the lateral and medial collateral ligaments respectively. Then the stress steadily decrease as the flexion angle augment until reaching respectively 3.07 and 0.00 MPa for the 70° flexion angle. At 40° flexion angle, the stress is balanced between the different ligaments, but for higher flexion angles it is focused in the cruciate ligaments. The stress in the cruciate ligaments starts lightly at 2.43 and 2.13 MPa for the anterior and posterior cruciate ligaments respectively in the standing position to reach a peak at the 55° flexion angle with stresses of 13.27 and 10.41 MPa.

4. Discussion

After the creation of the model and once the simulation were complete, the first step was to come back to the experimental data in order to make sure that our model was physiologically correct. In order to do so we compared the physiological position of the bones in the knee joint, given by EOS imaging, with their position obtained after a global knee equilibrium was reached in a simulation implemented with the same boundary conditions. The results were very satisfying. For the two lowest flexion angles they are even as good as they can get: the precision of our fitting of the 3D model on the EOS raw data is precise within 1 mm, meaning that after the equilibrium, an error on the tibia (only moving part of the model) of 2 mm is within that precision range and we cannot discriminate between an error brought by the simulation or an uncertainty in the aimed position. As a reminder, this precision corresponds to only two voxels in the data gathered on the MRI. Therefore, the simulation of the standing leg with a maximal distance of 0.7 mm is totally in its physiological position and the simulation at a 40° flexion angle, with 97% of its nodes at less than 2 mm of their experimental counterparts, is almost perfectly aligned with the experimental data. For the 55° flexion angle simulation, the final position of the bones is still very good; 81% are at most at twice our precision range, making it an acceptable error of position. However our model can be questioned for the simulation at a flexion angle of 70°. In this state, every node is at least at 4 mm of their aimed position. But in this particular case we noticed that this distance was mostly due to an anterior translation of the tibia. At this flexion angle, the tibia seams to start to slip, that would explain why our last simulation at the 85° flexion angle could not achieve equilibrium.

Our model may prove to be lacking some stability tools, like the menisci that would directly be in the way of such a translation. In that respect adding the menisci is the next step in our model. In two of the simulation we could also notice a slight rotation of the bone along its long axis. This may be due to the lack of contact between the ligaments and their surroundings. As the model is, nothing stops the cruciate ligaments to intersect each other, whereas physiologically they would twist one on the other and impede this rotation. However this kind of rotation was very small and to attend

to it may not be essential considering how this contact may make the model more complex. Adding a contact between the ligaments and the bone can also slightly change the way the lateral collateral ligament would work; adding a small lever arm on its tibia intersection and maybe making the whole knee joint a bit more stable. Once again we judge that the changes would prove to be to smalls to make this addition in our model a priority. Finally, the higher the flexion angle, the more the active stability may be impactful. Our model focus in the passive stability but maybe some active stability is mandatory for a global equilibrium at higher flexion angle, especially in this case were the knee is loaded. As the patella can be segmented on EOS images, a future model could involve a fitted patella, fixed in space as the femur, linked to the tibia with the patellar tendon.

This first model, however incomplete, still show some very physiological behavior. Beside the good bone position, we can see on the pressure maps that the points of highest pressure is in agreement with the contact path described by []. The pressure is rather well balanced between the two condyles, as expected from a healthy knee. Moreover, the slight overpressure on the external condyle showcases the different purpose of the two condyles: the internal condyle guiding the flexion while the external sustain a higher load. The stress in the ligaments also highlights the different functions of the ligaments. The collaterals ligaments guarantee the knee joint stability in extension while the cruciates take over in flexion. We can notice that usually it is the medial collateral ligament that is more loaded than the lateral; in this case it is the opposite because the volunteer suffer from a light varus (4.5°). The peak stress is also to be expected in the cruciate ligaments, it is due to the particular contact surfaces and the joint movement of translation and rotation in the knee joint. However, since the last simulation may be questionable, the peak stress can happen at higher flexion angle than what we observed here.

This model was built to be simple, and it showed that for low flexion angles it could achieve a global knee mechanical equilibrium that was perfectly physiological. For higher flexion angles the results

were promising but could be questionable. It will have to be completed in order to achieve a better stability. Thanks to this method which validates our model on the experimental data, here the bones positions, we know when we can be confident in the results obtained and when we have to be careful.

5. References

FIGURES

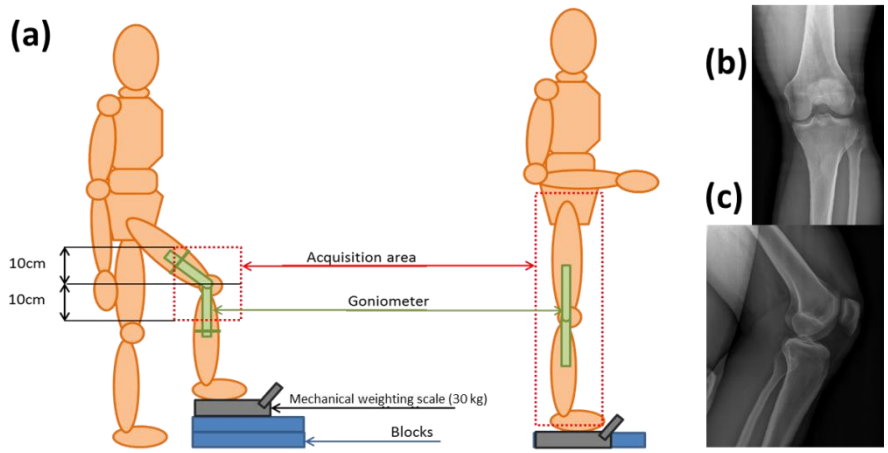

Fig. 1. (a) schematics of the EOS acquisition setup - side view . (b) Frontal scan of the knee at 55° of flexion – ie. 10 cm height step. (c) Matching sagittal scan of the knee.

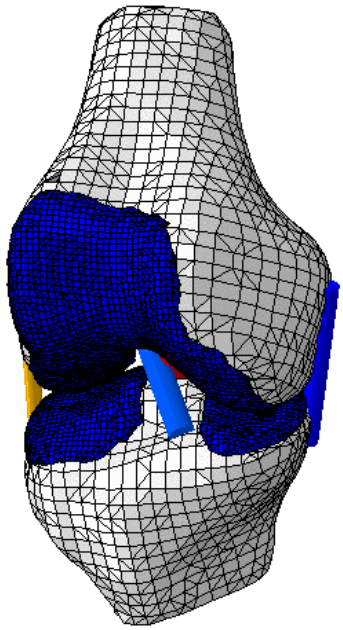

Fig. 2. Finite Element Model of the knee joint.

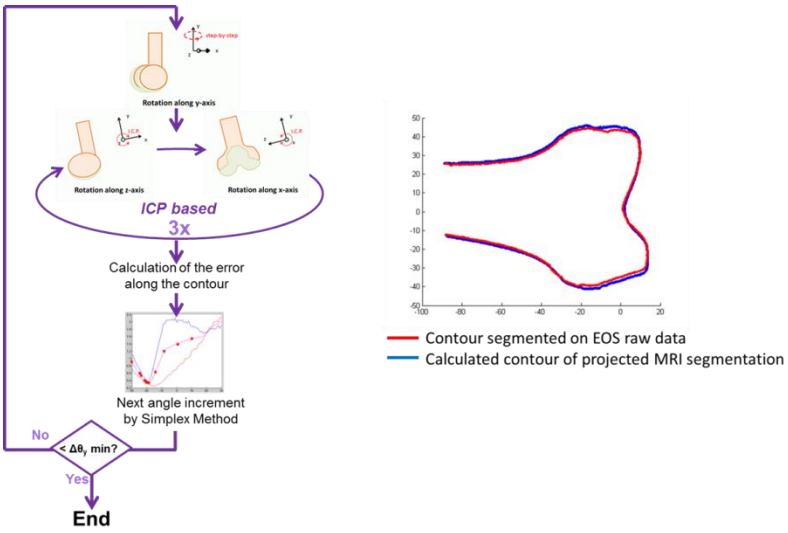

Fig. 3. Fitting algorithm of a 3D model on two 2D projections / Contour comparison of the femur at a 0° flexion angle

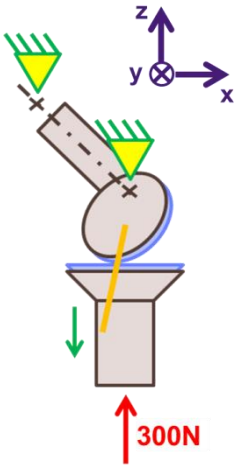

Fig. 4. FEA steps

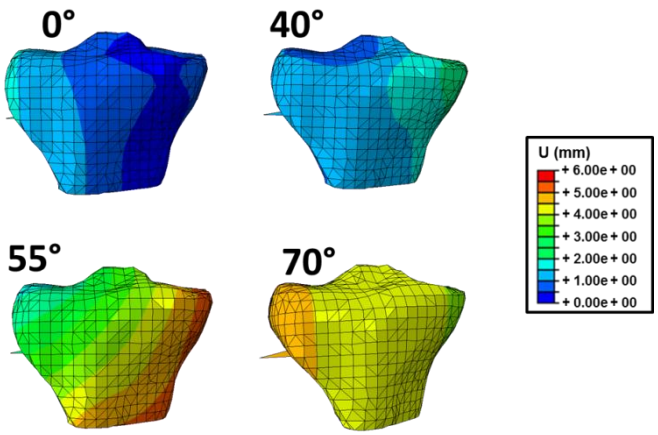

Fig. 5. Position distance of each node from the experimental data

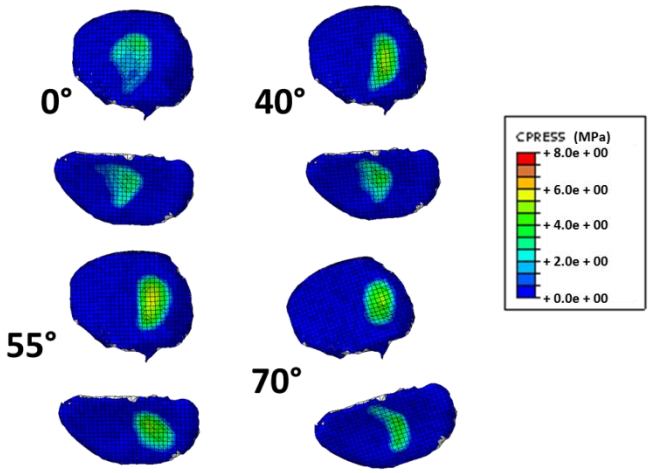

Fig. 6. Pressure map on tibia cartilages after global knee equilibrium

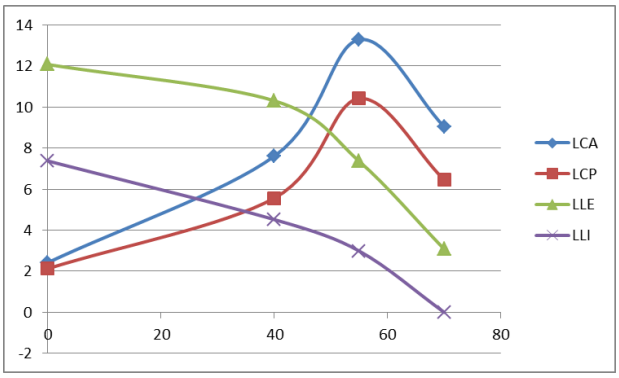

Fig. 7. Stress in the ligaments depending on the flexion angle